Journal of Biological Research

Bollettino della Società Italiana di Biologia Sperimentale

eISSN 2284-0230 - pISSN 1826-883

https://www.pagepressjournals.org/index.php/jbr/index

J Biol Res 2026 [Online ahead of print]

To cite this Article:
Ateş O, Kiraz Y. **Unraveling bortezomib resistance in multiple myeloma: insights from RNA-Seq and PI3K/mTOR pathway analysis.** *J Biol Res* doi: 10.4081/jbr.2026.14187

Submitted: 27 July 2025

Accepted: 4 December 2025

Early access: 4 February 2026

Unraveling bortezomib resistance in multiple myeloma: insights from RNA-Seq and PI3K/mTOR pathway analysis

Onur Ateş, Yağmur Kiraz

Faculty of Engineering, Department of Genetics and Bioengineering, İzmir University of Economics, Balçova, İzmir, Türkiye

Correspondence: Yağmur Kiraz, İzmir University of Economics, Faculty of Engineering, Department of Genetics and Bioengineering, Sakarya st. No:156 35330 Balçova, İzmir, Türkiye. Tel.: +90.2324888256 - E-mail: yagmur.kiraz@ieu.edu.tr

Key words: multiple myeloma, bortezomib-resistance, RNA-Seq, cross-resistance, Bez-235

Abstract

Multiple Myeloma (MM), characterized by abnormal plasma cell proliferation, lacks curative treatment due to drug resistance, notably against Bortezomib, a critical proteasome inhibitor. To elucidate resistance mechanisms, we conducted RNA sequencing on Bortezomib-sensitive and resistant RPMI-8226 MM cells, comparing them to healthy B-cells. Differential expression analysis highlighted significant alterations in immune signaling, proteasome function, and metabolism. Resistant MM cells exhibited decreased antigen-presentation genes (*HLA-DRA*, *HLA-DPA1*, *CD74*), indicating immune evasion. Downregulation of metabolic regulators like *GLUL* and *MDK* suggested a glycolytic metabolic shift, whereas enhanced proteasome activities and nucleocytoplasmic transport represented adaptive strategies against proteotoxic stress. Importantly, resistant cells showed notable upregulation of *PRAME* and *FAF1* genes, as

oncogenes and apoptosis-related genes linked to therapy resistance. Pathway analysis revealed enrichment in neurodegenerative disease-related pathways, suggesting common protein misfolding mechanisms in MM progression. Additionally, resistant cells displayed cross-resistance to the dual phosphoinositide 3-kinase (PI3K)/protein kinase B (AKT)/mammalian target of rapamycin (mTOR) inhibitor BEZ235, with a four-fold increase in IC_{50} values, reflecting enhanced survival signaling and metabolic flexibility. These findings underscore the multifaceted nature of Bortezomib resistance, driven by metabolic reprogramming, immune modulation, and translational regulation. Targeting these adaptive pathways through combination therapies involving proteasome inhibitors, metabolic modulators, and autophagy inhibitors may present novel strategies to overcome drug resistance in MM.

Introduction

Multiple Myeloma (MM) is a hematological malignancy originating from malignant B cells and characterized by the uncontrolled proliferation of abnormal plasma cells within the Bone Marrow (BM). These malignant plasma cells produce large amounts of abnormal monoclonal antibodies, contributing significantly to disease pathology.[1] Numerous gene mutations and chromosomal abnormalities have been associated with MM, further complicating its clinical management and therapeutic targeting.[2] MM is estimated to account for approximately 10% to 15% of all hematological malignancies and contributes to nearly 20% of deaths associated with hematological cancers.[3] Despite advancements in treatment, resistance to current therapeutic agents remains a significant clinical challenge.[4]

Bortezomib represents the most effective therapeutic agent currently used for the treatment of MM. Bortezomib is a boronate reversible inhibitor of the proteasome β5 catalytic subunit;

despite initial sensitivity, adaptive mechanisms and microenvironmental support frequently drive relapse and clinical resistance. Notably, de novo resistance to Bortezomib has also been observed in certain newly diagnosed MM patients prior to initiating their first treatment cycle.[5,6] In MM, recent studies have identified several specific resistance mechanisms, including proteasome subunit alterations, activation of alternative protein degradation pathways, metabolic reprogramming, and protective interactions with the bone marrow microenvironment.[7] Likewise, metabolic adaptations (such as a shift to glycolysis and redox alterations) and bone marrow stromal support have been shown to promote myeloma cell survival under drug pressure.[8,9] These diverse pathways often influence one another and collectively contribute to the multifactorial nature of drug resistance in MM.

Phosphoinositide 3-kinase (PI3K)/ protein kinase B (AKT)/ mammalian target of rapamycin (mTOR) signaling pathway has been shown to be essential in the development, advancement, and drug resistance mechanisms of MM. PI3K signaling is continuously activated in MM cells, aiding cell survival, growth, and resistance to therapies that induce apoptosis.[10] The initiation of this pathway has been associated with mutations in upstream regulators like receptor tyrosine kinases and oncogenic *Ras*, resulting in persistent PI3K-driven oncogenic signaling.[11] Moreover, preclinical studies in MM have shown that combining PI3K/Akt pathway inhibition with proteasome inhibitors such as Bortezomib can improve therapeutic effectiveness by overcoming drug resistance mechanisms.[10] Because MM cells depend on survival signals from stromal cells and cytokines in the bone marrow microenvironment, targeting PI3K disrupts these tumor–stromal interactions and can lead to a reduction in tumor burden.[12-13] In summary, these results emphasize the crucial importance of PI3K signaling in the advancement of MM and its resistance to therapy, pointing to its potential as a target for treatment.

In this study, we employed high-throughput RNA sequencing to identify the patterns of differentially expressed genes among healthy cells, MM cells, and MM cells resistant to Bortezomib. Through this approach, we determined specific molecular targets associated with Bortezomib-resistant MM cell lines, providing insights for overcoming drug resistance. Furthermore, pathway analysis prominently highlighted the PI3K/mTOR signaling axis in resistant cells, underscoring its potential as a therapeutic target. These findings were corroborated by *in vitro* validation experiments, reinforcing the clinical significance of targeting this pathway in MM therapy.

Materials and Methods

Cell lines and culture conditions

RPMI-8226, RPMI-8226/R were used as MMBortezomib-sensitive and Bortezomib-resistant cell lines, respectively and NCI-BL2171 cell lines were used for healthy B-cell control cell line. Cells were cultured in RPMI-1640 supplemented with 10% Fetal Bovine Serum (FBS) and 1% Penicillin/ Streptomycin(P/S) according to literature. Cells were grown in an incubator at 37°C with 5% CO_2.[14]

Generation of bortezomib-resistant cell line

The establishment of Bortezomib-resistant cell lines was conducted using a gradual exposure method. Bortezomib treatment commenced at an initial dose of 0.2 nM, with a stepwise increase of 0.2 nM every seven days. This dose escalation process was strictly controlled: the concentration was only increased if cell viability in culture exceeded a 70% threshold, as assessed via the trypan blue exclusion assay. This ensures the selection and adaptation of the

most resistant cells. Once the cells successfully adapted to growth in the presence of 14 nM Bortezomib, they were classified as RPMI-8226/R, with the drug concentration consistently maintained at 14 nM for the duration of the study.[15]

Cytotoxicity analysis

The cytotoxicity tests were conducted by the MTT (Thiazolyl blue tetrazolium bromide) assay. NCI-BL2171 healthy B-cell line, RPMI-8226 MMcell line and their Bortezomib-resistant derivative, RPMI-8226/R were plated in a 96-well plate at a density of 1×10^4 cells per well in 100 µL of RPMI media and treated with Bortezomib (at concentrations of 0 to 20 nM) and BEZ-235, a dual pan-class PI3K and mTOR inhibitor (at concentrations ranging from 0 to 2 µM) for 72 hours, based on preliminary experiments that established these doses as relevant for assessing cell viability (data not shown). For combination treatment experiments, Cells were then treated with increasing concentrations of Bortezomib (0–10 nM for RPMI-8226 MMcell line; 0–15 nM for RPMI-8226/R, Bortezomib-resistant RPMI-8226 derivative cell line) in the presence of matched increasing concentrations of BEZ235 (0–1000 nM for RPMI-8226; 0–1500 nM for RPMI-8226/R). Thus, both agents were co-titrated across the indicated ranges to evaluate the combined cytotoxic response. Single-agent controls were included for each drug at all corresponding concentrations. This approach was taken to determine the effect of PI3K/mTOR inhibition on the IC_{50} of Bortezomib in both sensitive and resistant lines. Subsequently, 20 µL of MTT solution (5 µg/mL) was added to each well and incubated for 4 hours. To solubilize the formazan crystals, 100 µL of Dimethyl Sulfoxide (DMSO) was added to each well. Absorbance readings were obtained using a spectrophotometer (Multiskan FC96 well plate Microplate Photometer, Cat#51119000, Thermo Scientific, Waltham, Massachusetts, USA) at 570 nm. Cell

viability assays were carried out in triplicate (n=3 biological replicates), with each experiment repeated independently at least three times.[16]

Total RNA isolation

Cells were seeded in 6-well-plate with a concentration of 3×10^5 cells/mL and treated with IC_{50} concentrations of Bortezomib determined for 72 hours. Total RNA isolation was performed with Invitrogen RNA Mini Kit (Cat#12183018A, Invitrogen, Carlsbad, CA, USA) according to the manual provided by the manufacturer.[17] Total RNA was isolated from four biological samples of each cell line to ensure reproducibility of the transcriptome data. RNA sequencing was performed on three independent biological replicates for each condition as follows: Healthy, Bortezomib sensitive and Bortezomib resistant.

RNA-Seq analysis

Sample quality control

Quality control of the isolated RNA material was performed using fluorometric and capillary electrophoresis methods to assess quantity, purity, and structural integrity. Measurements were conducted using the Qubit 3 Fluorometer (#Q33216, Thermo Fisher Scientific, Waltham, Massachusetts, USA) and the Agilent 2100 Bioanalyzer (#G2939BA, Agilent Technologies, Santa Clara, California, USA). Total RNA quality was assessed by Agilent 2100 Bioanalyzer (#G2939BA, Agilent Technologies, Santa Clara, California, USA), and only samples with a RIN (RNA Integrity Number) ≥ 7.0 were used for library preparation and sequencing.

Library preparation

The library preparation was carried out using the Illumina Total RNA Prep kit (#20040529, Illumina Inc., Qiagen, San Diego, California USA). The process involved removing ribosomal RNA from the total RNA, fragmenting the remaining RNA, and synthesizing primary and secondary cDNA strands. Steps such as ribosomal RNA removal, fragmentation, RNA purification, cDNA synthesis, addition of index and barcode sequences, and final purification were performed following the manufacturer's instructions.

RNA sequencing

RNA sequencing was performed on the Illumina NovaSeq 6000 platform (Illumina Inc., Qiagen, San Diego, California USA), targeting an average of 30 million paired-end (150 bp) reads per sample. Library quantification, dilution, and loading were executed per the manufacturer's guidelines.

Bioinformatics analysis

The cell lines used in the comparisons are referred to as follows: Healthy B-cells (NCI-BL2171), Bortezomib-sensitive MM cells (RPMI-8226), and Bortezomib-resistant MM cells (RPMI-8226/R). Raw reads were assessed with FastQC and trimmed with Trimmomatic v0.39. Cleaned reads were processed with the Illumina® DRAGEN RNA pipeline (Illumina Inc., Qiagen, San Diego, California USA), aligned to GRCh38.p13 with GENCODE v40 annotations, and summarized to gene-level counts. Downstream analyses used R 4.1 / Bioconductor.[18] Counts were filtered to retain genes with Count Per Million (CPM) > 1 in ≥ 2 samples and normalized by Trimmed Mean of M values (TMM). We fit a generalized linear model (edgeR) with a three-

level group factor (Healthy, Sensitive, Resistant) and tested contrasts for Healthy vs Sensitive, Healthy vs Resistant, and Sensitive vs Resistant. Differentially Expressed Genes (DEGs) were defined as Benjamini-Hochberg adjusted p value False Discovery Rate (FDR) < 0.05 and $\log_2$ fold change ($|\log_2 FC| \geq 1$.[19] For enrichment, we created directional gene sets (Up, Down) per contrast and ran topGO (Biological Process, Cellular Component, Molecular Function) and clusterProfiler Kyoto Encyclopedia of Genes and Genomes (KEGG) over-representation analyses with Benjamini–Hochberg False Discovery Rate (BH-FDR) correction ($q < 0.05$). Visualizations were generated with ggplot2 (volcano plots with $\log_2 FC$ cutoffs drawn at ±1; heatmaps limited to top 25–50 named genes per contrast).[20,22]

Statistical analysis

Statistical analyses were performed using R (v4.1) and GraphPad Prism (v10.3.1). For MTT assays, n = 3 biological replicates per condition were measured in technical triplicate. Dose–response curves were fit by nonlinear regression (four-parameter logistic) to estimate IC_{50} ± 95% Confidence Interval (CI). Group differences across doses were assessed by two-way Analysis of Variance (ANOVA) (genotype × dose) with Bonferroni correction; adjusted p values are reported on plots. RNA-seq statistics followed the edgeR workflow above (BH-FDR). Significance thresholds were at $p < 0.05$.

Results

Confirmation of bortezomib-resistance

In this study, we compared molecular responses to Bortezomib in RPMI-8226 and its resistant variant, RPMI-8226/R. Resistance was induced by gradually increasing Bortezomib

concentrations up to 14 nM. MTT assay confirmed the acquisition of resistance, showing an IC_{50} of 7.65 nM (%95 CI: 7.190 - 8.140 nM) in RPMI-8226 and 13.96 nM (%95 CI: 12.99 - 15.13 nM) in RPMI-8226/R, indicating a two-fold increase in resistance (Figure 1). Furthermore, the dose-response curve for RPMI-8226/R exhibited a significant rightward shift compared to RPMI-8226 (Two-Way ANOVA $p<0.0001$), demonstrating a robust resistance phenotype, particularly at low concentrations (<10 nM) where cell viability remained near 100%.

Differentially Expressed Genes (DEGs) analysis

To explore the transcriptional alterations associated with MM progression and the development of Bortezomib resistance, differential gene expression analysis was performed across three pairwise comparisons: i) healthy B-cells vs. Bortezomib-sensitive MM cells, ii) healthy B-cells vs. Bortezomib-resistant MM cells, and iii) Bortezomib-sensitive vs. Bortezomib-resistant MM cells. Table 1 represents the number of significantly Differentially Expressed Genes (DEGs) in each comparison.

The data reveal extensive transcriptomic changes across both disease progression and the development of resistance, particularly in pathways related to immune modulation, metabolism, and proteostasis. The data between healthy B-cells (NCI-BL2171) and Bortezomib-sensitive MM cells (RPMI-8226), marked shifts in gene expression, highlighting alterations characteristic of MM pathology. Several genes associated with antigen processing and presentation, including *CD74, HLA-DRA, HLA-DRB1*, and *HLA-DPA1,* were upregulated, suggesting enhanced MHC class II activity (Figure 2A-B).[21] Among these, *CD74* was particularly prominent. Additionally, immune-related molecules such as *CXCL10* and *JCHAIN* also exhibited elevated expression.[21] Marginal Zone B And B1 Cell Specific Protein (*MZB1*), a chaperone protein involved in plasma

cell differentiation and immunoglobulin folding, was also significantly upregulated. Insulin-like growth factor-binding protein 3 (*IGFBP3*), which modulates IGF signaling, showed strong expression and may support cell survival under stress (Table 2).[22] In parallel, downregulation of fetal hemoglobin genes such as *HBG2*, *HBE1*, and *HBG1* was noted, reflecting a shift in metabolic programming. *GATA1*, a regulator of hematopoiesis, was also suppressed. Notably, *PRAME*, an oncogene involved in immune regulation, and *FAF1*, an apoptosis-related gene, were also downregulated, potentially reflecting an adaptive stress response (Table 3).[23,24] The transcriptomic comparison between healthy B cells (NCI-BL2171) and Bortezomib-resistant MM cells (RPMI-8226/R) revealed numerous changes in gene expression. To identify molecular changes uniquely associated with acquired resistance, we focused on genes and pathways that distinguished the resistance from the sensitive MM cells.[25,26] In this context, genes such as *CX3CR1, ITGB7, MAF*, and *POU2AF1* were notably upregulated in resistant cells, suggesting roles in cell adhesion, microenvironmental adaptation, and altered transcriptional regulation specific to acquired Bortezomib resistance (Figure 2C-D). These changes point to altered differentiation and metabolic states in MM cells. Compared to healthy B-cells, resistant RPMI-8226/R cells exhibited additional shifts beyond the shared MM signature, including upregulation of *CX3CR1, MAF, ITGB7* and *CHST4,* suggestive of altered microenvironmental interaction and transcriptional control, alongside reduced expression of several immune-surveillance genes. When comparing RPMI-8226 to RPMI-8226/R, we observed several gene expression alterations that may contribute to acquired resistance. Genes involved in cell adhesion and microenvironmental interaction, such as *CX3CR1, ITGB7, CHST4*, and *RAI2*, were upregulated.[27–29] Transcription factors associated with MM biology, such as *MAF* and *POU2AF1,* were also increased in resistant cells (Table 2).[27] Conversely, several genes involved

in immune surveillance and protein degradation were downregulated. Reductions in *HLA-DQA1, HLA-DQA2, HLA-DRB1, CCL19,* and *CXCL10* point to impaired immune visibility.[30,31] Downregulation of *UBD*, a regulator of ubiquitin-dependent degradation, may indicate a shift in proteostasis under Bortezomib-induced stress (Table 3).

In both MM lines relative to healthy B-cells, we observed a shared core of directionally consistent DEGs that likely reflects typical myeloma biology. Notably, *MZB1, JCHAIN*, and *IGFBP3* were consistently upregulated, consistent with plasma-cell chaperoning and survival signaling, whereas fetal hemoglobin cluster genes (*HBG1/2*, *HBE1*) were downregulated.

Gene Ontology (GO) analysis

To identify the biological pathways altered in MM progression and Bortezomib resistance, Gene Ontology (GO) enrichment analysis was performed on DEGs to focus on biologically significant changes[32] (Figure 3; Supplementary Materials S4). Importantly, GO enrichments were interpreted separately for upregulated and downregulated gene sets, analogous to the approach later used for KEGG pathways. In the transition from healthy B-cells to Bortezomib-sensitive MM cells (Figure 3A; Supplementary Materials S4A), upregulated pathways were enriched for immune response, regulation of immune system processes, defense response, and cell adhesion, with CC localization primarily in the cell periphery and extracellular region, extracellular vesicle, and plasma membrane. MF terms were dominated by signaling receptor binding and activity as well as molecular transducer activity, and immune receptor activities. Downregulated genes were enriched for regulation of localization, homeostatic processes and telomerase localization (Figure 3D; Supplementary Materials S4D). CC terms were related to extracellular exosomes, organelles, secretory vesicles, and membrane-bounded organelles, while MF

enrichment highlighted structural molecule activity, chromatin and channel activities. These immune related alterations indicate a loss or attenuation of key B-cell immune functions in the myeloma cells.[33-35] In the comparison between NCI-BL2171and drug-resistant RPMI-8226/R cells, upregulated pathways were enriched for immune response, regulation of immune system processes, defense response, and cell adhesion, with CC localization primarily in the extracellular region, extracellular vesicle, and plasma membrane (Figure 3B; Supplementary Materials S4B). MF terms were dominated by signaling receptor activity, molecular transducer activity, and ion channel–related functions. Downregulated genes were enriched for organonitrogen compound biosynthesis, peptide biosynthesis, small molecule metabolic processes, and nucleoside phosphate biosynthesis (Figure 3E; Supplementary Materials S4E). CC terms were related to extracellular exosomes, secretory vesicles, and membrane-bounded organelles, while MF enrichment highlighted structural molecule activity, protein binding, and hydrolase activity. These findings suggest that resistant MM cells not only share the structural and receptor-level adaptations of their sensitive counterparts, but also activate heightened proteostasis and stress-mitigation mechanisms to withstand chronic Bortezomib exposure (a hallmark of acquired drug resistance).[32,36] Lastly, comparing drug-sensitive RPMI-8226 to resistant RPMI-8226/R cells, upregulated genes in resistant cells were strongly enriched for ribosome biogenesis, rRNA metabolic processes, RNA processing, and translation-related pathways (Figure 3C; Supplementary Materials S4C). CC terms pointed to ribonucleoprotein complexes, ribosomal subunits, and intracellular organelle lumens, with MF enrichment in RNA binding, nucleic acid binding, and ribosome binding, reflecting elevated protein synthesis machinery in resistant cells. Downregulated genes showed enrichment for cytoplasmic translation, regulation of programmed cell death, immune system processes, and apoptotic

pathways (Figure 3F; Supplementary Materials S4F). CC terms were predominantly extracellular, including extracellular space, extracellular region, and extracellular membrane-bounded organelles. MF terms included structural constituent of ribosome, cytokine activity, and receptor ligand activity, suggesting reduced immune-related signaling and translational structural functions in resistant cells.

Overall, separating upregulated and downregulated GO terms revealed clear and biologically meaningful differences between sensitive and resistant cell states, highlighting activated translational programs in resistant cells and altered immune and signaling pathways across all comparisons.

Pathway analysis

To identify coordinated molecular changes contributing to MM progression and Bortezomib resistance, we performed KEGG pathway enrichment analysis across three comparisons (Figure 4). In the transition from healthy B cells to MM, upregulated pathways included protein processing in the endoplasmic reticulum, antigen processing and presentation, and oxidative phosphorylation, indicating increased proteotoxic stress and reliance on degradation mechanism, consistent with the known vulnerability of MM cells to proteasome inhibitors like Bortezomib[37,38] (Figure 4A). Enrichment of viral related pathways, such as Epstein-Barr virus infection, further suggests active immune signaling in the early stage of MM (Figure 4B). In parallel, downregulated pathways included nucleocytoplasmic transport and steroid biosynthesis, suggesting remodeling of translational activity and metabolic regulation.

Resistant cells showed upregulation of pathways such as N-Glycan biosynthesis, cellular senescence, and proteasome function, indicating enhanced protein folding quality control and cell cycle regulation compared to healthy B cells[39,40] (Figure 4C). Meanwhile, downregulated pathways prominently featured the ribosome, oxidative phosphorylation, and carbon metabolism, suggesting translational repression and a shift towards glycolytic metabolism, an adaptive survival strategy in resistant myeloma[41,42] (Figure 4D).

When directly comparing sensitive and resistant MM cells, the most enriched upregulated pathway was the proteasome, with 24 of 46 genes upregulated, reflecting compensatory degradation activity.[43] Additional enriched pathways included DNA replication, mismatch repair, and nucleocytoplasmic transport, indicating increased reliance on RNA processing and trafficking.[44,45] (Figure 4E) Conversely, downregulated pathways included ribosome biogenesis, antigen processing, oxidative phosphorylation, and p53 signaling, consistent with translational suppression, immune evasion, and metabolic reprogramming[41,42] (Figure 4F). The changes in DEG signatures reflect and align with the GO/KEGG profiles observed for the resistant comparison (Figure 3B; Supplementary Materials S4B; Figure 4C–D), reinforcing a phenotype of proteostasis/stress adaptation and niche-interaction remodeling (Tables 2–3; Supplementary materials S1-S3). In both MM lines relative to healthy B-cells, we observed a shared core of directionally consistent DEGs that likely reflects typical myeloma biology as detailed in the current paper. This shared signature co-occurs with enrichments in proteostasis- and matrix/adhesion-related terms, as captured by GO/KEGG, and provides a baseline MM transcriptomic context against which the resistant-specific changes can be interpreted (Figure 2A–D; Fig. 3–4; Supplementary materials S1–S3).

Taken together, these results highlight a dual resistance signature of upregulation of proteasome activity and RNA/protein quality control pathways, alongside suppression of ribosome, oxidative phosphorylation, and immune-related signaling. This combination suggests that Bortezomib-resistant MM cells adapt through both enhanced protein degradation and immune evasion, consistent with previously reported mechanisms of resistance.

Cross-resistance development against BEZ-235

To identify pathway-level alterations associated with MM and drug resistance, we examined the expression patterns of genes within the PI3K/mTOR signaling pathway across the three pairwise comparisons. After applying the $|FC| \geq 1$ and adjusted $p < 0.05$ thresholds, 32 genes were identified as significantly dysregulated. These genes are summarized in Table 4 and visualized in Figure 5. In both sensitive and resistant MM lines relative to NCI-BL2171healthy B cells, a consistent set of pathway components displayed marked upregulation. These included *BCL2, CCND1, SIK1, PRKCZ, FOXO3, CDK9, NPTN,* and *CERK,* reflecting broad activation of pro-survival, mitogenic, and PI3K-linked signaling programs in MM cells.[46-48] Downregulated genes in these comparisons included metabolic and structural regulators such as *BCAT1*, *TRPM4, PRKCB, SKP2, RFK* and *HSP90B1* several of which showed consistent suppression across both MM lines.[46-49] The resistant line (RPMI-8226/R) showed a highly similar DEG pattern to the sensitive line (RPMI-8226) when compared to NCI, with additional upregulation of *RBL2* and *PWP2*, suggesting an enhanced cell-cycle regulatory signature associated with resistance (Table 4).

When directly comparing resistant and sensitive MM cells, a smaller subset of pathway components met significance criteria. Four genes (*CERK, NIFK, PWP2,* and *TTLL4*) were

significantly upregulated in resistant cells, suggesting their potential involvement in the adaptive or compensatory signaling associated with resistance acquisition. Conversely, several core PI3K/mTOR and survival-related genes (including *BCL2, CCND1, PRKCZ, FOXO3, PIM3, MCL1, CDK6, PDK1,* and *GSK3B*) were significantly downregulated in RPMI-8226/R relative to RPMI-8226 (Table 4). Also Figure 5 presents a heatmap of all 32 significantly dysregulated pathway genes. Together, these results indicate that while MM cells share a conserved activation signature involving multiple PI3K/mTOR pathway components, resistant cells display additional selective alterations that may contribute to drug tolerance mechanisms.

To test the effect of PI3K/mTOR inhibition, cells were treated with BEZ235. BEZ-235 response differed markedly between Bortezomib-sensitive and -resistant RPMI cells, with IC_{50} increasing from 400 nM to 1.6 μM a four-fold rise indicating a possible cross-resistance (Figure 6A). Exposure of MMcells to increasing concentrations of BEZ235 revealed a pronounced difference in drug sensitivity between the parental RPMI-8226 line and the Bortezomib-resistant RPMI-8226/R variant (Figure 6A). While RPMI-8226 cells exhibited a dose-dependent reduction in viability across the 0–2000 nM range, the resistant cells remained largely refractory to BEZ235, showing only a modest decline at the highest concentrations. When both drugs were titrated simultaneously, co-treatment markedly enhanced cytotoxicity in the parental line, producing a leftward shift in the viability curve compared with Bortezomib alone (Figure 6B–C). In contrast, RPMI-8226/R cells displayed minimal sensitization under the same conditions, with viability remaining high at low and intermediate doses and decreasing only at the highest dual-drug concentrations (Figure 6B, 6D). Direct comparison of Bortezomib alone versus the combination demonstrated a clear reduction in the apparent IC_{50} in RPMI-8226 cells, whereas the resistant cells maintained a substantially attenuated shift, highlighting their cross-resistant phenotype.

Collectively, these findings indicate that while BEZ235 potentiates the cytotoxic effects of Bortezomib in sensitive MM cells, this cooperative interaction is significantly blunted in the resistant counterpart. Collectively, these data demonstrate significant and direction-specific dysregulation of the PI3K/mTOR axis in resistant cells, supporting the observed cross-resistance between Bortezomib and PI3K/mTOR inhibition and strengthening the rationale for co-treatment to overcome resistance. Despite PI3K/AKT/mTOR being a key survival pathway in MM, RNA-Seq revealed various signaling activation in resistant cells, suggesting alternative resistance mechanisms such as enhanced proteasome activity or altered protein transport. These suggest that RPMI-8226/R cells avoid apoptosis and develop drug resistance via different pathways. Upregulation of proteasome activity and protein transportation might cause resistant development on these cell lines without AKT upregulation.[54,50] These findings indicate that several PI3K/mTOR pathway genes are differentially expressed between Bortezomib-sensitive and -resistant cells, suggesting that alterations in this signaling axis may contribute to the development of proteasome inhibitor resistance. The discussion section includes the mechanistic implications of these changes as below.

Discussion

The emergence of resistance to Bortezomib represents a critical barrier to effective MM treatment, reflecting the capacity of malignant plasma cells to remodel core biological processes in response to proteasome inhibition. By integrating transcriptomic profiling across healthy, drug-sensitive, and drug-resistant states, our study provides mechanistic insight into the coordinated adaptations that enable survival despite sustained proteotoxic stress. One of the clearest hallmarks observed across the disease progression axis was the attenuation of antigen

presentation and immune surveillance pathways. Downregulation of HLA class II molecules, including *HLA-DRA, HLA-DPA1, HLA-DRB1*, and *CD74,* suggests a progressive reduction in immunogenicity from healthy B cells to Bortezomib-resistant MM cells. This immune evasion strategy aligns with the known immunosuppressive phenotype of advanced MM, where reduced antigen presentation can impair recognition by $CD4^+$ T cells and antigen-presenting cell interactions.[36] Furthermore, important inflammatory cytokines like *CXCL10* and *IL32* demonstrated notable downregulation, strengthening the idea that resistant cells purposefully inhibit immune signaling pathways to improve their survival. Second, the data point to a significant metabolic reprogramming. The downregulation of oxidative phosphorylation along with the simultaneous upregulation of pathways linked to glycolysis and cellular stress responses indicates a transition towards a Warburg-like metabolism.[41] This metabolic adjustment likely enables resistant cells to meet their bioenergetic requirements while reducing oxidative damage, thus supporting prolonged survival during proteotoxic stress.

When directly comparing the sensitive and resistant MM cells (RPMI-8226 *vs*. RPMI-8226/R), the focus shifts to core adaptive strategies employed to survive chronic proteasome inhibition. The enhancement of proteasome-related pathways (Figure 4E) underscores the compensatory proteostasis strategies that MM cells utilize to counter proteasome inhibition, probably by increased autophagic flux and different protein degradation pathways.[43,51] Our findings align with previous observations in similar myeloma models. For instance, Rückrich *et al.* reported comparable patterns of proteasome subunit upregulation and sustained proteasome activity in Bortezomib-adapted MMcells, supporting our transcriptomic results and underscoring the consistency of these molecular adaptations across independent studies.[51] In addition to *PRAME*, which was emphasized in previous sections due to its strong signal and prognostic associations,

our dataset also identified significant downregulation of *FAF1*. *FAF1* encodes Fas-associated factor 1, a multifunctional protein that promotes apoptosis through death receptor signaling and participates in proteasomal regulation. Its reduced expression in resistant cells may attenuate apoptosis and support survival under proteotoxic stress, suggesting that *FAF1* could represent an additional modulator of Bortezomib sensitivity.[57,58] Counterintuitively, ribosomal function was markedly reduced in resistant cells (Figure 4F), signifying an adaptive strategy to save energy and reduce proteotoxic stress, a common feature in treatment-resistant cancer cells. This repression probably signifies an adaptive strategy to save energy and reduce proteotoxic stress, frequently seen in cancer cells resistant to treatment.[52] In contrast, the enhancement of nucleocytoplasmic transport and mRNA surveillance pathways indicates a mechanism to preserve protein homeostasis by selectively removing damaged RNA and proteins for degradation.

A notable finding was the development of cross-resistance to BEZ-235, a dual PI3K/mTOR inhibitor, in Bortezomib-resistant MM cells. Our results showed a four-fold rise in the IC_{50} value of BEZ235 in resistant cells, indicating that the molecular changes granting Bortezomib resistance also confer tolerance to PI3K/mTOR inhibition. This cross-resistance is probably fueled by increased PI3K/AKT/mTOR signaling and metabolic adaptability, highlighting the necessity for combination therapy approaches to avert resistance emergence.[53] Nevertheless, we acknowledge that our current evidence only partially supports a definitive conclusion of cross-resistance, as it is based mainly on IC_{50} and viability assays. Future functional studies will be required to validate this link and confirm whether PI3K/mTOR inhibitors consistently lose efficacy in Bortezomib-resistant settings. Beyond PI3K/mTOR targeting, other therapeutic strategies have been proposed to overcome proteasome inhibitor resistance in multiple myeloma.

One approach is to interfere with alternative protein quality control pathways, such as heat shock protein 90 (*HSP90*) inhibition or modulation of autophagy; for instance, the HSP90 inhibitor IPI-504 has been shown to reverse Bortezomib resistance in MM models.[54] Another promising direction is targeting mitochondrial metabolism, since resistant cells often rely on oxidative phosphorylation and metabolic rewiring for survival; mitochondrial metabolic dysregulation has been implicated in MM disease progression and treatment resistance.[55] Inhibitors that impair mitochondrial function or alter redox balance have shown potential in preclinical PI-resistant models. In addition, emerging immunotherapies, including CAR-T cells, bispecific antibodies, and immune checkpoint blockade, have demonstrated robust efficacy in patients with relapsed and PI-resistant myeloma.[56]

While our study primarily focused on transcriptomic alterations driving cross-resistance to Bortezomib and BEZ235, these complementary approaches highlight the broader therapeutic landscape and suggest that integrating pathway-directed treatments with immunotherapy may provide a more durable response in PI-resistant disease. Our findings highlight roles for immune evasion, metabolism, translation, and proteostasis in resistance. While promising, these results are based on the RPMI-8226 model and require validation in other cell lines and patient-derived samples for clinical relevance. In addition, our conclusions are primarily derived from transcriptomic (RNA-seq) data. Although RNA-seq provides valuable insights into gene expression changes, it does not fully capture post-transcriptional regulation or protein-level alterations. Therefore, future studies integrating proteomic profiling, functional assays, and *in vivo* validation will be essential to confirm the biological significance of these findings and to strengthen their translational relevance. Moreover, our results align with the most recent literature, which emphasizes that Bortezomib resistance in MM arises from the interplay of

proteasome adaptation, metabolic rewiring, and immune evasion. Recent reviews have specifically highlighted the central role of PI3K/AKT/mTOR signaling and stress-response pathways in sustaining resistant phenotypes, as well as the need for combination approaches to overcome adaptive survival mechanisms.[41,59] By integrating transcriptomic alterations in these same pathways, our study not only supports these observations but also extends them by providing direct evidence from resistant versus sensitive myeloma cells.

Conclusions

In this study, we provide a comprehensive transcriptomic and functional characterization of Bortezomib resistance in MMusing healthy B cells, Bortezomib-sensitive RPMI-8226 cells, and their resistant derivative. Our findings demonstrate that resistance arises through coordinated alterations in immune regulation, metabolism, proteostasis, and translational control. Resistant cells exhibited pronounced downregulation of antigen-presentation and immune-surveillance genes, suggesting progressive immune evasion as the disease advances. Concurrent suppression of oxidative phosphorylation and ribosomal pathways, together with enhanced proteasome activity, nucleocytoplasmic transport, and RNA-processing machinery, reflects a shift toward stress-tolerant, energy-conserving survival programs under chronic proteotoxic pressure. Importantly, PI3K/mTOR-related genes displayed significant but selective dysregulation, and functional assays revealed a four-fold increase in the IC_{50} of the PI3K/mTOR inhibitor BEZ235 in resistant cells, indicating the emergence of cross-resistance. These results suggest that although PI3K/mTOR signaling remains active in MM biology, resistant cells acquire additional compensatory mechanisms, such as elevated proteostasis capacity and altered metabolic wiring, that diminish reliance on canonical PI3K/mTOR survival cues.

Taken together, our data highlight a multifaceted resistance architecture in MM, driven by the interplay of immune modulation, metabolic reprogramming, translational remodeling, and enhanced protein-quality control. These findings support the rationale for therapeutic strategies that combine proteasome inhibition with agents targeting metabolic adaptation, autophagy, or RNA/protein surveillance pathways. Future studies involving proteomic validation, mechanistic perturbation, and patient-derived samples will be essential to translate these insights into clinically actionable approaches for overcoming proteasome inhibitor resistance in multiple myeloma.

References

1. Alexander DD, Mink PJ, Adami HO, et al. Multiple myeloma: a review of the epidemiologic literature. Int J Cancer 2007;120:40-61.
2. Morgan GJ, Walker BA, Davies FE. The genetic architecture of multiple myeloma. Nat Rev Cancer 2012;12:335-48.
3. Fairfield H, Falank C, Avery L, Reagan MR. Multiple myeloma in the marrow: pathogenesis and treatments: Understanding the pathogenesis of multiple myeloma. Ann N Y Acad Sci 2016;1364:32-51.
4. Kingsley LA, Fournier PGJ, Chirgwin JM, Guise TA. Molecular biology of bone metastasis. Mol Cancer Ther 2007;6:2609-17.
5. Schmitt SM, Deshmukh RR, Dou QP. Proteasome inhibitors and lessons learned from their mechanisms of action and resistance in human cancer. In: Resistance to Targeted Anti-Cancer Therapeutics. Springer International Publishing; 2014:1-46.
6. Maiso P, Huynh D, Moschetta M, et al. Metabolic signature identifies novel targets for drug resistance in multiple myeloma. Cancer Res 2015;75:2071-82.
7. Saavedra-García P, Roman-Trufero M, Al-Sadah HA, et al. Systems level profiling of chemotherapy-induced stress resolution in cancer cells reveals druggable trade-offs. Proc

Natl Acad Sci U S A 2021;118:e2018229118.

8. Schwestermann J, Besse A, Driessen C, Besse L. Contribution of the tumor microenvironment to metabolic changes triggering resistance of multiple myeloma to proteasome inhibitors. Front Oncol 2022;12:899272.

9. Pelon M, Krzeminski P, Tracz-Gaszewska Z, Misiewicz-Krzeminska I. Factors determining the sensitivity to proteasome inhibitors of multiple myeloma cells. Front Pharmacol 2024;15:1351565.

10. Ikeda H, Hideshima T, Fulciniti M, et al. PI3K/p110{delta} is a novel therapeutic target in multiple myeloma. Blood 2010;116:1460-68.

11. Ramakrishnan V, Kumar S. PI3K/AKT/mTOR pathway in multiple myeloma: from basic biology to clinical promise. Leuk Lymphoma 2018;59:2524-34.

12. Heinemann L, Möllers KM, Ahmed HMM, et al. Inhibiting PI3K-AKT-mTOR signaling in multiple myeloma-associated mesenchymal stem cells impedes the proliferation of multiple myeloma cells. Front Oncol 2022;12:874325.

13. Piddock RE, Bowles KM, Rushworth SA. The role of PI3K isoforms in regulating bone marrow microenvironment signaling focusing on acute myeloid leukemia and multiple myeloma. Cancers (Basel) 2017;9:29.

14. Akcora-Yildiz D, Gonulkirmaz N, Ozkan T, et al. HIV-1 integrase inhibitor raltegravir promotes DNA damage-induced apoptosis in multiple myeloma. Chem Biol Drug Des 2023;102:262-70.

15. Xing H, Yang X, Liu T, et al. The study of resistant mechanisms and reversal in an imatinib resistant Ph+ acute lymphoblastic leukemia cell line. Leuk Res 2012;36:509-13.

16. Fan Y, Chiu JF, Liu J, et al. Resveratrol induces autophagy-dependent apoptosis in HL-60 cells. BMC Cancer 2018;18:581.

17. Rump LV, Asamoah B, Gonzalez-Escalona N. Comparison of commercial RNA extraction kits for preparation of DNA-free total RNA from Salmonella cells. BMC Res Notes 2010;3:211.

18. Bolger AM, Lohse M, Usadel B. Trimmomatic: a flexible trimmer for Illumina sequence data. Bioinformatics 2014;30:2114-20.

19. Robinson MD, McCarthy DJ, Smyth GK. edgeR: a Bioconductor package for differential expression analysis of digital gene expression data. Bioinformatics 2010;26:139-40.

20. Adrian Alexa JR. topGO. Bioconductor; 2017. doi:10.18129/B9.BIOC.TOPGO

21. Yang J, Wang F, Chen B. HLA-DPA1 gene is a potential predictor with prognostic values in multiple myeloma. BMC Cancer 2020;20:915.

22. Bieghs L, Johnsen HE, Maes K, et al. The insulin-like growth factor system in multiple

myeloma: diagnostic and therapeutic potential. Oncotarget 2016;7:48732-52.

23. Chen Z, Luo HY, Basran RK, et al. A T-to-G transversion at nucleotide -567 upstream of HBG2 in a GATA-1 binding motif is associated with elevated hemoglobin F. Mol Cell Biol 2008;28:4386-93.

24. Olthof SG, Fatrai S, Drayer AL, et al. Downregulation of signal transducer and activator of transcription 5 (STAT5) in CD34+ cells promotes megakaryocytic development, whereas activation of STAT5 drives erythropoiesis. Stem Cells 2008;26:1732-42.

25. Meeuwsen MH, Wouters AK, Wachsmann TLA, et al. Broadly applicable TCR-based therapy for multiple myeloma targeting the immunoglobulin J chain. J Hematol Oncol 2023;16:16.

26. Chanukuppa V, Paul D, Taunk K, et al. Proteomics and functional study reveal marginal zone B and B1 cell specific protein as a candidate marker of multiple myeloma. Int J Oncol 2020;57:325-37.

27. Zhao C, Inoue J, Imoto I, et al. POU2AF1, an amplification target at 11q23, promotes growth of multiple myeloma cells by directly regulating expression of a B-cell maturation factor, TNFRSF17. Oncogene 2008;27:63-75.

28. Lou X, Deng W, Shuai L, et al. RAI2 acts as a tumor suppressor with functional significance in gastric cancer. Aging (Albany NY) 2023;15:11831-44.

29. Han J, Deng H, Lyu Y, et al. Identification of N-glycoproteins of knee cartilage from adult osteoarthritis and Kashin-Beck disease based on quantitative glycoproteomics, compared with normal control cartilage. Cells 2022;11:2513.

30. Deitiker P, Oshima M, Jankovic J, Atassi MZ. Influences of HLA DRB1, DQA1 and DQB1 on T-cell recognition of epitopes and of larger regions of the botulinum neurotoxin molecule. Immunol Lett 2017;190:257-64.

31. Yan Y, Chen R, Wang X, et al. CCL19 and CCR7 expression, signaling pathways, and adjuvant functions in viral infection and prevention. Front Cell Dev Biol 2019;7:212.

32. Zhou P, Zhang C, Song X, et al. ΔNp63α promotes Bortezomib resistance via the CYGB-ROS axis in head and neck squamous cell carcinoma. Cell Death Dis 2022;13:327.

33. Wu Q, Yang Z, Nie Y, et al. Multi-drug resistance in cancer chemotherapeutics: mechanisms and lab approaches. Cancer Lett 2014;347:159-66.

34. Sengsayadeth S, Malard F, Savani BN, et al. Posttransplant maintenance therapy in multiple myeloma: the changing landscape. Blood Cancer J 2017;7:e545.

35. Zhou J, Zhang M, Zhang Y, et al. Identification of potential prognostic biomarker for predicting survival in multiple myeloma using bioinformatics analysis and experiments. Front Genet 2021;12:722132.

36. Zisi A, Bartek J, Lindström MS. Targeting ribosome biogenesis in cancer: Lessons learned and way forward. Cancers (Basel) 2022;14:2126.

37. Chauhan D, Hideshima T, Anderson KC. Proteasome inhibition in multiple myeloma: therapeutic implication. Annu Rev Pharmacol Toxicol 2005;45:465-76.

38. Gozzetti A, Papini G, Candi V, et al. Second generation proteasome inhibitors in multiple myeloma. Anticancer Agents Med Chem 2017;17:920-26.

39. Albert B, Kos-Braun IC, Henras AK, et al. A ribosome assembly stress response regulates transcription to maintain proteome homeostasis. Elife 2019;8:45002

40. Aronson LI, Davies FE. DangER: protein ovERload. Targeting protein degradation to treat myeloma. Haematologica 2012;97:1119-30.

41. Weir P, Donaldson D, McMullin MF, Crawford L. Metabolic alterations in multiple myeloma: From oncogenesis to proteasome inhibitor resistance. Cancers (Basel) 2023;15:1682.

42. Zaal EA, Wu W, Jansen G, et al. Bortezomib resistance in multiple myeloma is associated with increased serine synthesis. Cancer Metab. 2017;5(1):7.

43. Di Lernia G, Leone P, Solimando AG, et al. Bortezomib treatment modulates autophagy in multiple myeloma. J Clin Med 2020;9:552.

44. Turner JG, Dawson J, Sullivan DM. Nuclear export of proteins and drug resistance in cancer. Biochem Pharmacol 2012;83:1021-32.

45. Tye BW, Commins N, Ryazanova LV, et al. Proteotoxicity from aberrant ribosome biogenesis compromises cell fitness. Elife 2019;8:e43002.

46. Nag S, Qin J, Srivenugopal KS, et al. The MDM2-p53 pathway revisited. J Biomed Res 2013;27:254-71.

47. Huang J, Dibble CC, Matsuzaki M, Manning BD. The TSC1-TSC2 complex is required for proper activation of mTOR complex 2. Mol Cell Biol 2008;28:4104-15.

48. Tsai PJ, Lai YH, Manne RK, et al. Akt: a key transducer in cancer. J Biomed Sci 2022;29:76.

49. Nelson ED, Benesch MG, Wu R, et al. High EIF4EBP1 expression reflects mTOR pathway activity and cancer cell proliferation and is a biomarker for poor breast cancer prognosis. Am J Cancer Res 2024;14:227-42.

50. Ri M, Iida S, Nakashima T, et al. Bortezomib-resistant myeloma cell lines: a role for mutated PSMB5 in preventing the accumulation of unfolded proteins and fatal ER stress. Leukemia 2010;24:1506-12.

51. Rückrich T, Kraus M, Gogel J, et al. Characterization of the ubiquitin-proteasome system in Bortezomib-adapted cells. Leukemia 2009;23:1098-05.

52. Brancolini C, Iuliano L. Proteotoxic stress and cell death in cancer cells. Cancers (Basel) 2020;12:2385.

53. Browne IM, Okines AFC. Resistance to targeted inhibitors of the PI3K/AKT/mTOR pathway in advanced oestrogen-receptor-positive breast cancer. Cancers (Basel) 2024;16:2259.

54. Roué G, Pérez-Galán P, Mozos A, et al. The Hsp90 inhibitor IPI-504 overcomes Bortezomib resistance in mantle cell lymphoma in vitro and in vivo by down-regulation of the prosurvival ER chaperone BiP/Grp78. Blood 2011;117:1270-79.

55. Nair R, Gupta P, Shanmugam M. Mitochondrial metabolic determinants of multiple myeloma growth, survival, and therapy efficacy. Front Oncol 2022;12:1000106.

56. Rendo MJ, Joseph JJ, Phan LM, DeStefano CB. CAR T-Cell therapy for patients with multiple myeloma: Current evidence and challenges. Blood Lymphatic Cancer Targets Ther 2022;12:119-36.

57. Park MY, Ryu SW, Kim KD, et al. Fas-associated factor-1 mediates chemotherapeutic-induced apoptosis via death effector filament formation. Int J Cancer 2005;115:412-18.

58. Yu C, Kim BS, Kim E. FAF1 mediates regulated necrosis through PARP1 activation upon oxidative stress leading to dopaminergic neurodegeneration. Cell Death Differ 2016;23:1873-85.

59. Tyrna P, Procyk G, Szeleszczuk Ł, Młynarczuk-Biały I. Different strategies to overcome resistance to proteasome inhibitors-A summary 20 years after their introduction. Int J Mol Sci 2024;25:8949.

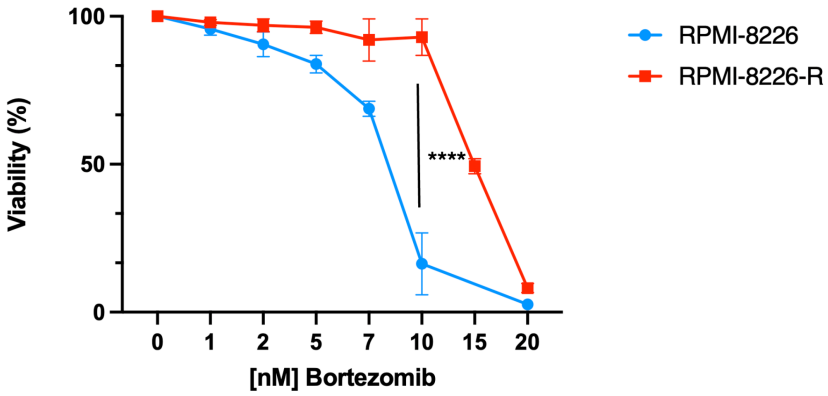

Figure 1. Cell Viability (%) of RPMI-8226 (Sensitive) and RPMI-8226/R (Resistant) cells following Bortezomib treatment. Bortezomib was administered for 72 hours, and cell viability

was evaluated using the MTT assay. The experiments were conducted in triplicate, and error bars represent the standard deviation. Statistical significance: $p < 0.0001$ (****).

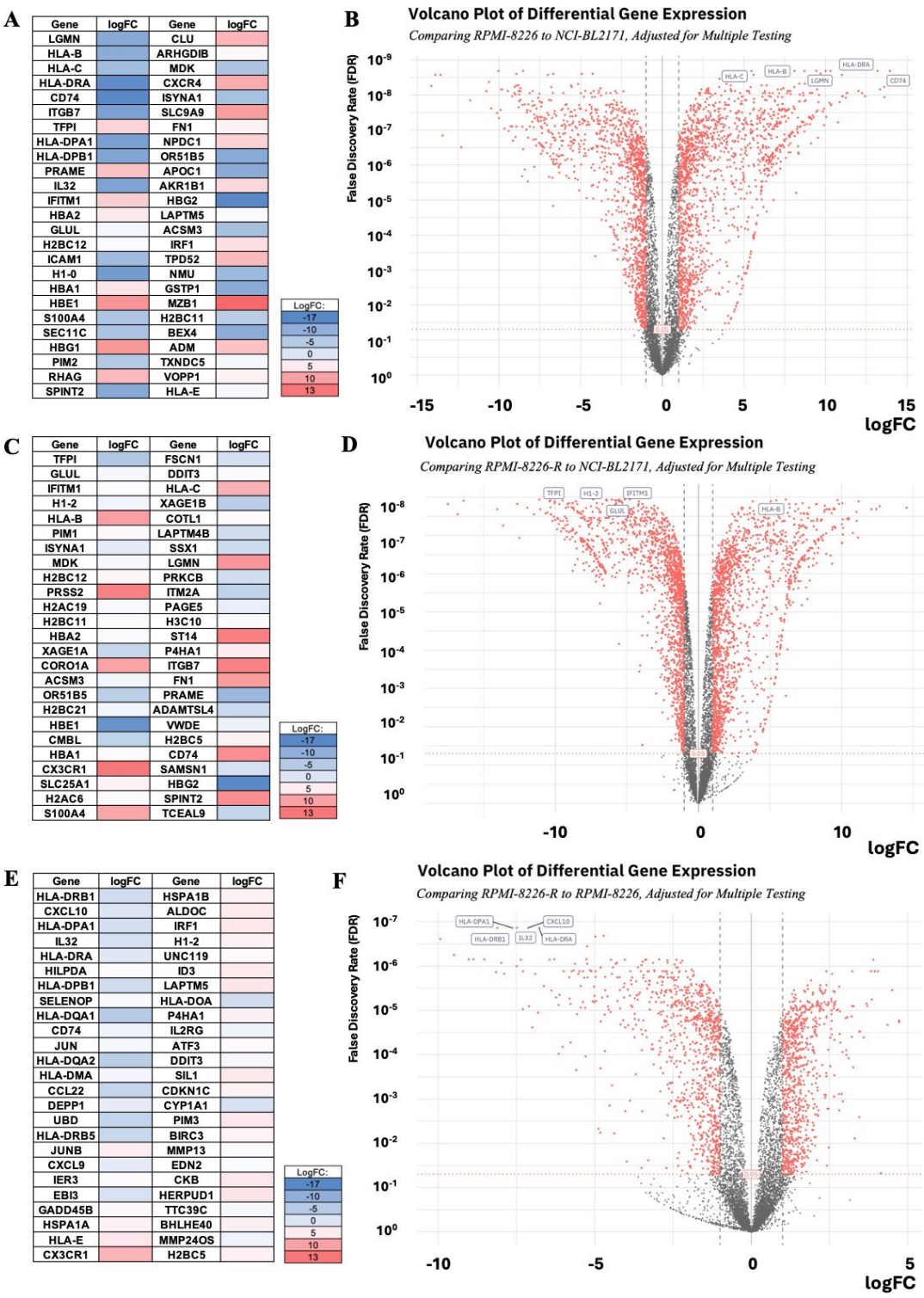

Figure 2. Differential gene expression in multiple comparisons. Panels A, C, E show heatmaps of the top 50 up- and down-regulated genes, and panels B, D, F show volcano plots of gene

expression changes. Comparisons: (A, B) Healthy B cells (NCI-BL2171) *vs*. Bortezomib-sensitive MM (RPMI-8226); (C, D) Healthy B *vs*. Bortezomib-resistant MM (RPMI-8226/R); (E, F) Bortezomib-sensitive *vs*. Bortezomib-resistant MM. In the heatmaps, color intensity reflects relative expression (row Z-score), with blue indicating downregulation and red indicating upregulation. In the volcano plots, each point represents a gene (gray for non-significant, colored for significant genes). The volcano plots include a horizontal line at the significance threshold (adjusted p value = 0.05) and vertical lines at $\log_2$-fold change = ±1 for reference. Genes meeting the significance criteria (false discovery rate < 0.05) are highlighted. Labels denote select genes of interest. Heatmaps were generated in Excel, and Volcano plots were generated in R Studio.

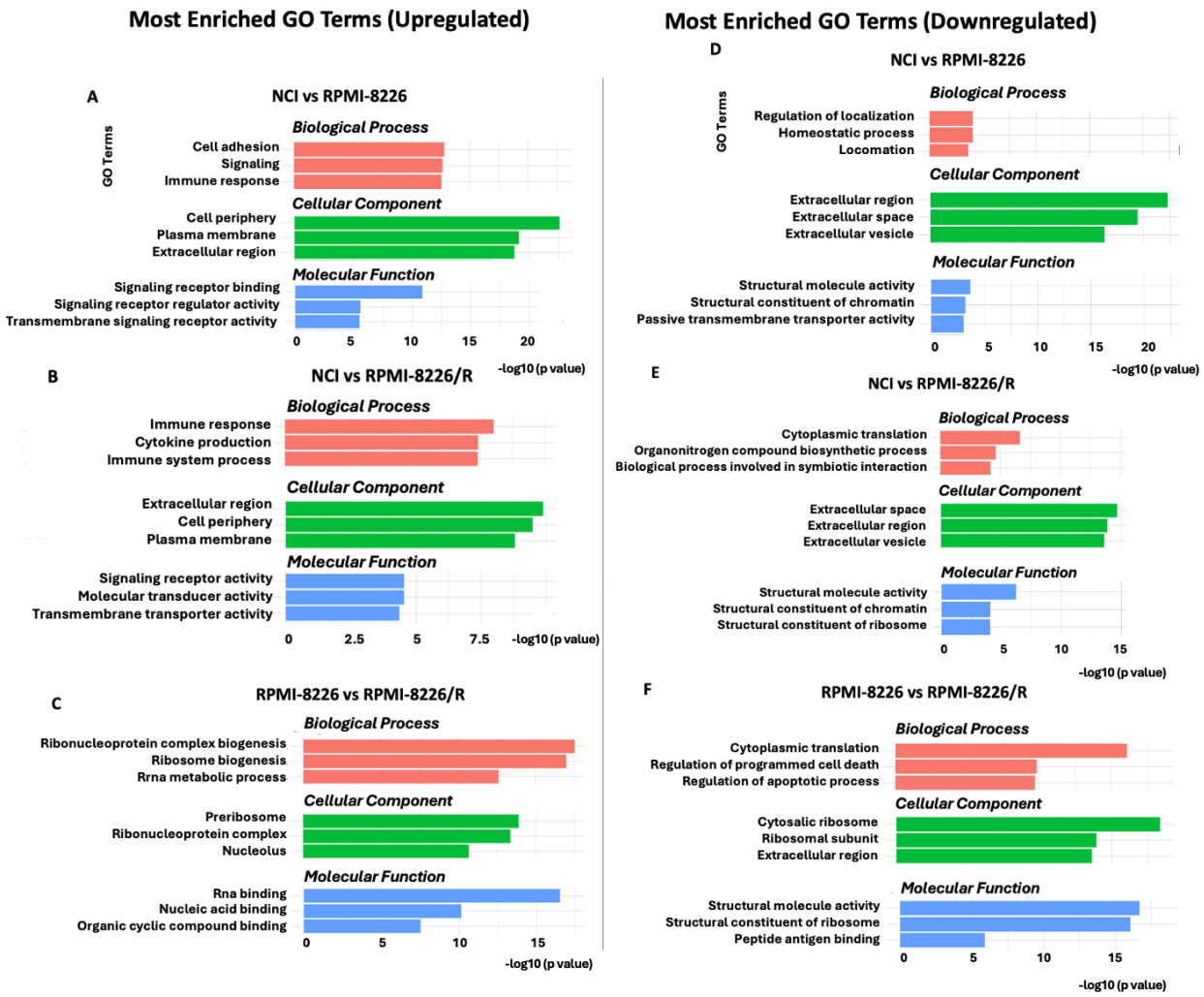

Figure 3. Gene Ontology (GO) enrichment analysis of upregulated and downregulated genes across the three pairwise comparisons. GO analysis was performed separately for upregulated (top panel: A–C) and downregulated (bottom panel: D–F) differentially expressed genes (DEGs) for each comparison: NCI-BL2171*vs* RPMI-8226 (A, D), NCI-BL2171*vs* RPMI-8226/R (B, E), and RPMI-8226 vs RPMI-8226/R (C, F). For each comparison, red bars indicate significantly enriched Biological Process (BP), green bars Cellular Component (CC), and blue bars Molecular Function (MF) (adjusted $p < 0.05$). Lower p values indicating greater enrichment significance. The enrichment analysis was performed using a hypergeometric test, and significance thresholds

were set at $p < 0.05$. Bars depict individual GO terms, with the length of each bar directly proportional to enrichment significance (smaller p values have longer bars). This figure provides a summarized overview of the most significantly enriched Gene Ontology (GO) terms, while the complete enrichment results are presented in Supplementary Material S4.

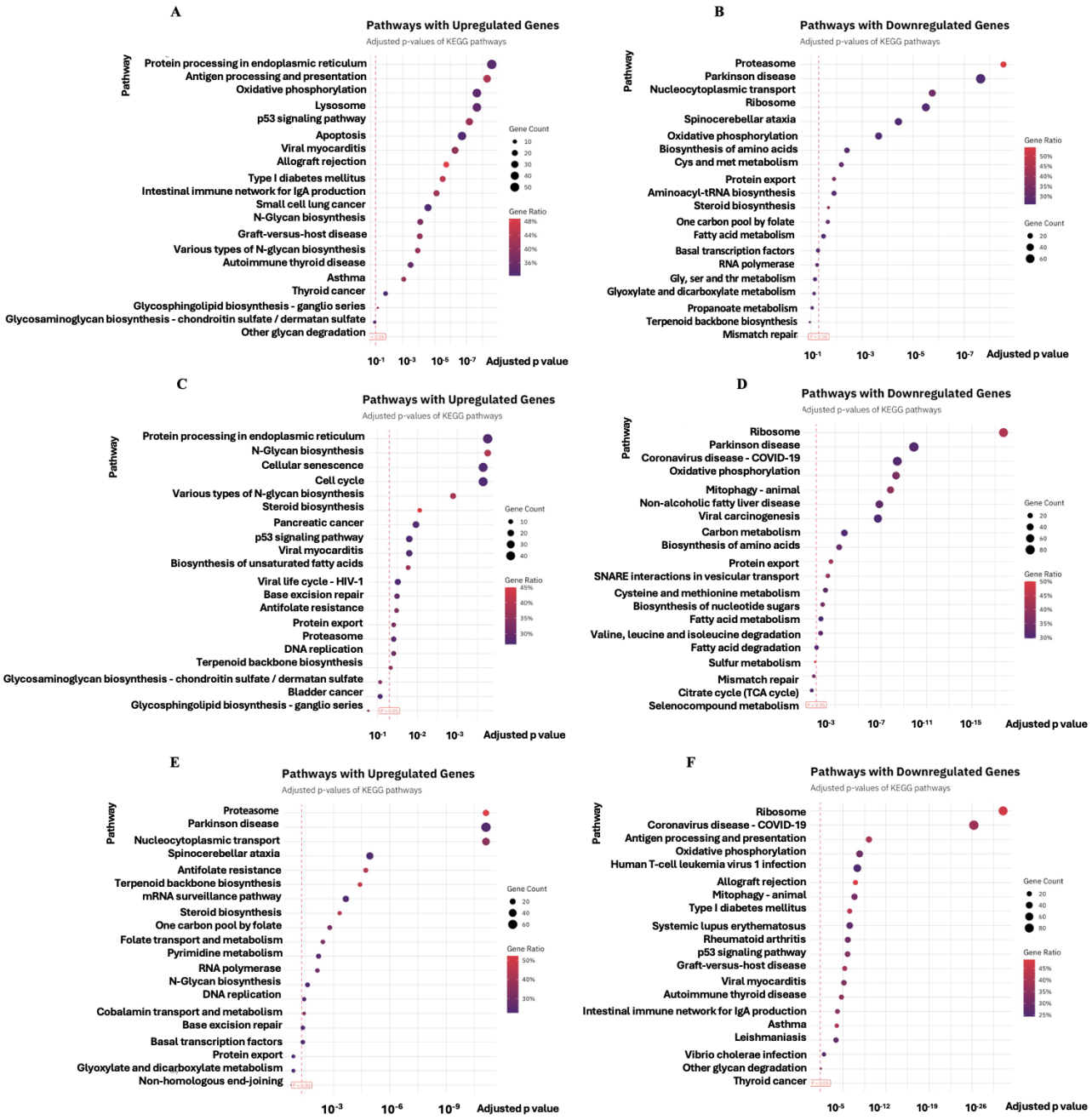

Figure 4. Kyoto Encyclopedia of Genes and Genomes (KEGG) pathway enrichment analysis of significantly upregulated and downregulated genes across three pairwise comparisons of healthy, drug-sensitive, and drug-resistant multiple myeloma cells. (A, B) NCI-BL2171 (healthy B-cells) vs. RPMI-8226 (Bortezomib-sensitive MM cells), (C, D) NCI-BL2171 *vs*. RPMI-8226/R (Bortezomib-resistant MM cells) and (E, F) RPMI-8226 vs. RPMI-8226/R. Panels A, C, E

display pathways enriched in upregulated genes, while panels B, D, F show pathways enriched in downregulated genes. Enrichment analysis was performed using the KEGG database. Significance was assessed using a hypergeometric test with Benjamini–Hochberg-adjusted p values (FDR). Only pathways with adjusted p values below 0.05 were retained and ranked. Each dot represents an individual enriched pathway, where: The x-axis shows the adjusted p value (–$\log_{10}$ scale), The y-axis lists pathway names (shortened for clarity), Dot size indicates the number of differentially expressed genes associated with each pathway (Gene Count), Dot color corresponds to Gene Ratio (*i.e.*, proportion of genes from the pathway found in the DEG list).

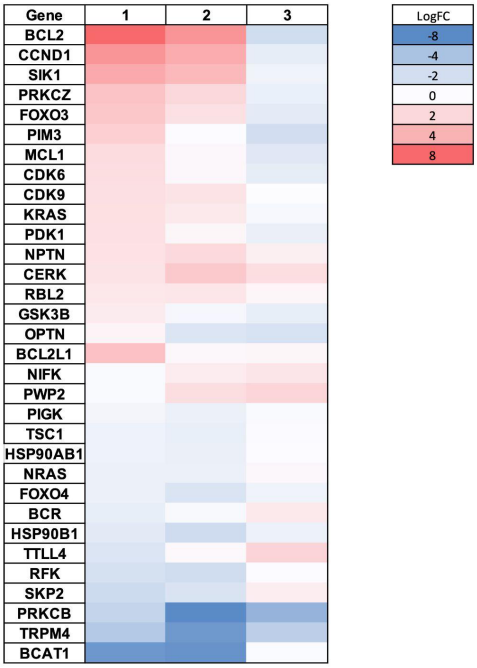

Figure 5. Heatmap of significantly dysregulated genes in the mTOR signaling pathway across the three pairwise comparisons. The heatmap displays the 32 significantly dysregulated genes (adjusted $p < 0.05$) belonging to the mTOR signaling pathway. Columns represent the three comparisons: (1) MM Sensitive vs NCI, (2) MM Resistant vs NCI, and (3) MM Resistant vs MM Sensitive. Rows correspond to individual pathway genes. Colors represent log2 fold-change

(LogFC) values (-8 to +8) according to the scale shown on the right, where red denotes upregulation and blue denotes downregulation. Only genes meeting statistical significance thresholds are included; non-significant pathway members have been excluded for clarity.

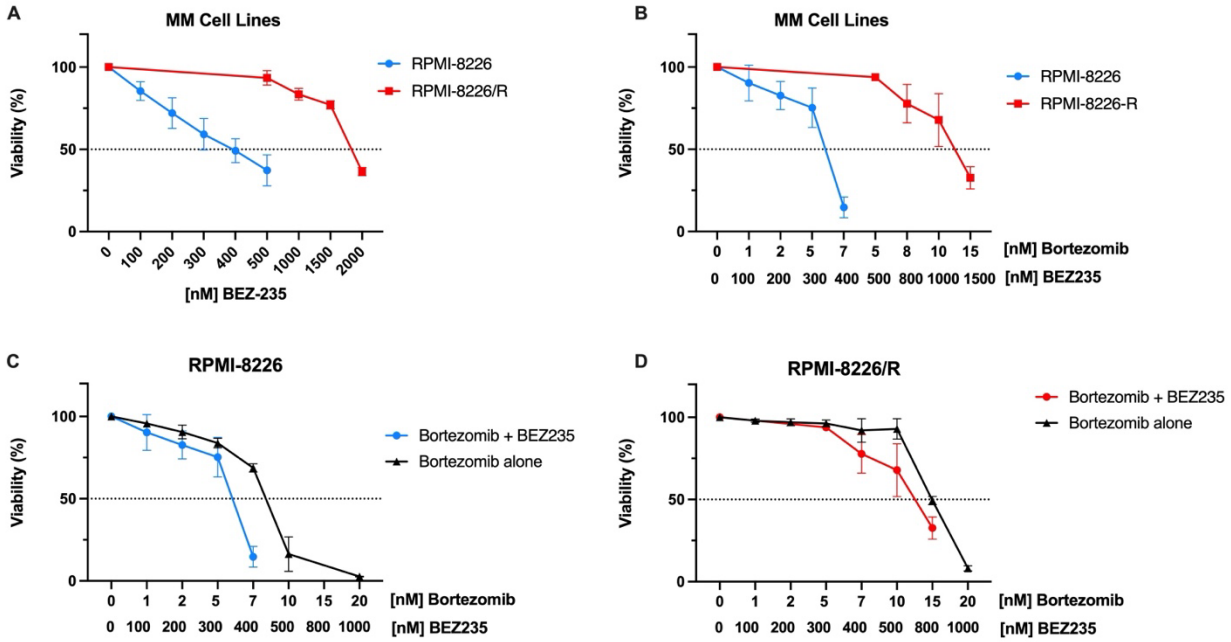

Figure 6. Differential cytotoxic responses of parental and Bortezomib-resistant MM cells to BEZ-235 and combination treatment. (A) Dose–response curves of RPMI-8226 and RPMI-8226/R multiple myeloma cell lines treated with increasing concentrations of BEZ-235 (0–2000 nM) for 48 h. (B) Combined treatment with Bortezomib (0–15 nM) and BEZ-235 (0–1500 nM) in RPMI-8226 and RPMI-8226/R cells. (C) Synergistic effect of BEZ-235 + Bortezomib in parental RPMI-8226 cells. The dotted line indicates 50% viability. (D) Co-treatment response of RPMI-8226/R resistant cells. Data are presented as mean ± SD of at least three independent experiments.

Table 1. Comparison groups and number of genes showing significant changes.*

Test	Control	Experiment	Number of Downregulated Genes	Number of not Changed Genes	Number of Upregulated Genes
1	NCI-BL2171	RPMI-8226	2150	3354	2292
2	NCI-BL2171	RPMI-8226/R	2433	2991	2372
3	RPMI-8226	RPMI-8226/R	1687	4539	1570

**Downregulated: Fold Change (FC) < –1; Upregulated: FC > +1; Unchanged: –1 ≤ FC ≤ +1.*

Table 2. Top20 Upregulated genes for all comparisons. 1) NCI-BL2171 vs RPMI-8226, 2) NCI-BL2171 vs RPMI-8226/R and 3) RPMI-8226 vs RPMI-8226/R (This table shows the Top-20 upregulated differentially expressed genes (DEGs) by $\log_2$ fold change ($\log_2$FC) for summary purposes. Full DEGs lists for each comparison, ranked by adjusted p value and including $\log_2$FC, p value, and expression metrics, are provided in Supplementary materials S1–S3.

1) NCI-BL2171vs RPMI-8226		**2) NCI-BL2171vs RPMI-8226/R**		**3) RPMI-8226 vs. RPMI-8226/R**	
Gene	**$\log_2$FC**	**Gene**	**logFC**	**Gene**	**$\log_2$FC**
CD74	13.94	*JCHAIN*	14.54	*RAI2*	4.73
JCHAIN	13.60	*MZB1*	12.67	*CHST4*	4.72
MZB1	13.58	*PVALB*	12.43	*FSTL4*	4.50
CXCL10	13.33	*IGFBP3*	12.08	*KEL*	4.36
HLA-DRA	13.17	*CX3CR1*	11.20	*RAB32*	4.14
PVALB	12.41	*MAF*	11.15	*RNF182*	4.05
LSP1	12.23	*CDKN2A*	11.06	*IGFBP2*	3.95
HLA-DRB1	12.00	*CD8B*	11.05	*CX3CR1*	3.90
CD8B	11.33	*LSP1*	10.80	*TMEM72*	3.85

MAL	11.28	*PCP4*	10.50	*CNN3*	3.83
IGFBP3	11.23	*CXCL6*	10.49	*TNNI3K*	3.71
CDKN2A	11.05	*KRT7*	10.40	*LPGAT1*	3.69
KRT7	11.01	*POU2AF1*	10.11	*ZC3H4*	3.59
H1-0	11.00	*SPP1*	10.09	*MRM1*	3.47
HLA-DQA1	10.85	*MAL*	10.08	*IFITM1*	3.46
SPP1	10.75	*ST14*	10.07	*CTAG2*	3.45
TSTD1	10.34	*CYP24A1*	10.05	*MAGEA12*	3.31
AZGP1	10.32	*UNC13C*	10.03	*CD72*	3.27
HLA-DPA1	10.29	*CBR3*	10.02	*HPS6*	3.26
MAF	10.23	*ITGB7*	9.82	*LBH*	3.23

Table 3. Top20 Downregulated genes for all comparisons. 1) NCI-BL2171 vs RPMI-8226, **2)** NCI-BL2171 vs RPMI-8226/R and **3)** RPMI-8226 vs RPMI-8226/R. (This table shows the Top-20 downregulated differentially expressed genes (DEGs) for summary purposes. Full DEGs lists for each comparison, ranked by adjusted p value and including log fold change (log_2FC), p value, and expression metrics, are provided in Supplementary materials S1–S3.

1) NCI-BL2171vs RPMI-8226		**2) NCI-BL2171vs RPMI-8226/R**		**3) RPMI-8226 vs. RPMI-8226/R**	
Gene	**log_2FC**	**Gene**	**logFC**	**Gene**	**log_2FC**
HBG2	-14.14	*HBG2*	-17.49	*HLA-DQA1*	-9.93
HBE1	-13.89	*HBG1*	-16.81	*HLA-DQA2*	-9.50
HBG1	-13.57	*HBE1*	-16.40	*UBD*	-9.02
HBZ	-13.45	*GSTP1*	-14.05	*CCL22*	-8.87
GYPA	-11.76	*HBZ*	-13.65	*HLA-DRB5*	-8.52

CA1	-10.77	*PRAME*	-12.66	*HSPA6*	-8.15
RHAG	-10.62	*GYPA*	-11.96	*HLA-DRB1*	-8.11
GYPB	-10.48	*CA1*	-11.49	*HLA-DPB1*	-7.99
MYL4	-10.12	*TFPI*	-11.11	*HLA-DOA*	-7.98
PRAME	-10.03	*RHAG*	-11.04	*HLA-DQB1*	-7.90
FAF1	-10.00	*GYPB*	-10.68	*HLA-DPA1*	-7.64
HEMGN	-9.90	*APOC1*	-10.55	*CYP1A1*	-7.49
CMBL	-9.86	*XAGE1B*	-10.40	*IL32*	-7.49
RHOXF2B	-9.82	*OR51B5*	-10.34	*EBI3*	-7.36
PPP1R14A	-9.67	*GDF15*	-10.33	*MT2A*	-7.29
CTCFL	-9.46	*RHOXF2B*	-10.32	*HLA-DQB2*	-7.29
GATA1	-9.40	*BEX4*	-10.29	*CXCL10*	-7.13
MS4A3	-9.29	*FAF1*	-10.19	*EDIL3*	-7.10
GYPE	-9.19	*HEMGN*	-10.10	*CCL19*	-7.00

Table 4. Significantly dysregulated genes related to the Phosphoinositide 3-kinase (PI3K)/mammalian target of rapamycin (mTOR) PI3K/mTOR pathway within each comparison group.

Comparison	**Upregulated Genes**	**Downregulated Genes**
1) RPMI-8226 - NCI-BL2171	*BCL2, CCND1, SIK1, PRKCZ, FOXO3, PIM3, MCL1, CDK6, CDK9, KRAS, PDK1, NPTN, CERK*	*BCAT1, TRPM4, PRKCB, SKP2, RFK, TTLL4, HSP90B1, BCR, FOXO4, NRAS*
2) RPMI-8226/R - NCI	*BCL2, CCND1, SIK1, PRKCZ, FOXO3, CDK9, NPTN, RBL2, CERK, PWP2*	*BCAT1, TRPM4, PRKCB, SKP2, RFK, HSP90B1, FOXO4, HSP90AB1, TSC1, PIGK, OPTN*
3) RPMI-8226/R-RPMI-8226	*CERK, NIFK, PWP2, TTLL4*	*BCL2, CCND1, PRKCZ, FOXO3, PIM3, MCL1, CDK6, PDK1,*

		GSK3B, OPTN, PRKCB, TRPM4

Contributions: Onur Ateş, data curation, investigation, methodology, visualization, writing – original draft; Yağmur Kiraz, conceptualization, funding acquisition, supervision, validation, writing – review and editing.

Conflict of interest: the authors have no conflict of interest to declare.

Availability of data and materials: statistical summaries are presented in the published article. The data sets generated or analyzed during the present study are available in the NCBI GEO repository will be available upon publication.

Acknowledgement: this work has been supported as part of the 2022-03 numbered Project approved by Izmir University of Economics Scientific Research Projects Commission. We also thank Dr. Can Holyakin for his support with the bioinformatics analyses and data visualization.

Online supplementary materials

Sheet 1: NCI-BL2171 vs RPMI-8226 DEG List

Sheet 2: NCI-BL2171 vs RPMI-8226-R DEG List

Sheet 3: RPMI-8226 vs RPMI-8226-R DEG List

Sheet 4: Gene Ontology (GO) Enrichment Analysis of Upregulated and Downregulated Genes Across the Three Pairwise Comparisons

Sheet 5: Dose-Dependent and Significant Effects of Bez235 on RPMI-8226 Cell Viability